Criticality in the dynamic failure model

2008 J. Phys. A: Math. Theor. 41 145101

(http://iopscience.iop.org/1751-8121/41/14/145101)

J. Phys. A: Math. Theor. **41** (2008) 145101 (7pp) doi:10.1088/1751-8113/41/14/145101

Criticality in the dynamic failure model

J Jo[1], H Kang[1], M Y Choi[1,2], J Choi[3] and B-G Yoon[4]

[1] Department of Physics and Astronomy, Seoul National University, Seoul 151-747, Korea
[2] Asia-Pacific Center for Theoretical Physics, Pohang 790-784, Korea
[3] Department of Physics, Keimyung University, Daegu 704-701, Korea
[4] Department of Physics, University of Ulsan, Ulsan 680-749, Korea

E-mail: bgyoon@ulsan.ac.kr

Received 1 December 2007, in final form 6 February 2008
Published 26 March 2008
Online at stacks.iop.org/JPhysA/41/145101

Abstract

To probe the interplay of different mechanisms for criticality, we study the dynamic failure model, each element of which is allowed to break or to be healed with given conditional probabilities. Under an external load the system evolves to the stationary state, which may exhibit breakages of various sizes. In addition, as the healing parameter is varied, the system undergoes a discontinuous transition between the functioning state and the failed one. In the regimes with appropriate amounts of healing and fluctuations of the surviving fraction, scale invariance in spatial and temporal correlations is observed, manifested by the power spectrum of the breakage rate of elements and by the cluster size distribution of broken elements.

PACS numbers: 89.75.Da, 87.18.Bb, 05.65.+b

Many phenomena in nature exhibit power-law behavior in spatial and/or temporal correlations. Well-known examples include the frequency-size distribution of earthquakes known as the Gutenberg–Richter law [1], various distributions in biological systems [2], degree distributions in complex networks [3] and time series in several systems [4]. The concept of self-organized criticality (SOC), proposed with the help of a sandpile model [5], attempts to provide a theoretical explanation of power-law scaling behavior from a unified viewpoint. According to the idea of SOC, the system is brought into the critical state through the interplay of the input from outside and dissipation present in the system. As a consequence, small perturbations give rise to avalanches of all sizes, thus resulting in power-law distributions. Note that the steady input from outside, which acts as 'healing' in the system, plays a key role in attaining criticality in SOC. While this idea has been applied to a variety of phenomena [6], there also exists cases of power-law scaling not belonging to this category: among typical examples are breakdown phenomena involving discontinuous phase transitions, which contrasts with the SOC mechanism [7].

In understanding the general mechanism of power-law scaling, it is thus desirable to compare the contrasting frameworks and to probe the precise role of healing in criticality. For this purpose, this paper studies a model system in which both frameworks are present, namely, a dynamical system exhibiting stationary states with power-law behavior and transitions between the stationary states as the system parameters vary. To be specific, we adopt the recently proposed dynamic failure model [8], which incorporates healing effects into the fiber bundle models for breakdown in heterogeneous materials [9–11]. The dynamic failure model, proposed to describe, e.g., the evolution of dysfunction and possible failure in a living organism, resulting from the interplay of cell damage/death and cure/birth, has been observed to exhibit many desirable properties as to the time evolution to the stationary state and the lifetime under applied load [8, 12]. For a given healing parameter, the system tends to resist external load for a rather long time, followed by sudden failure with some fraction of elements still surviving, if the load exceeds a transition value depending on the healing parameter. Otherwise there is no breakdown, indicating that the system-wide failure is governed by the interplay of healing and external load. Furthermore, in some range of the healing parameter, there exist two stable stationary states, between which the system undergoes a discontinuous phase transition. In consequence, as the healing parameter is varied, there arises a hysteresis. We carry out Monte Carlo (MC) simulations of the system with local load sharing (LLS) to observe that, for appropriate ranges of the system parameters, size distributions of clusters of broken elements as well as power spectra of the breakage rate of elements exhibit power-law behavior. Such critical behavior of spatial and temporal correlations apparently arise from the interplay of discontinuous transitions as well as SOC.

We consider a system consisting of N elements under external load F. Each element has its own threshold and endures the load below the threshold. The element may become broken, however, if the threshold is exceeded. We assign 'spin' variables to these in such a way that $\sigma_i = \pm 1$ for the ith element broken/intact. The state of the system is then described by the configuration of all the elements, $\boldsymbol{\sigma} \equiv (\sigma_1, \sigma_2, \ldots, \sigma_N)$. We are interested in how the average number of intact elements, $\bar{x} = (1 + \bar{\sigma})/2$ with $\bar{\sigma} \equiv N^{-1} \sum_j \sigma_j$, evolves in time as well as its stationary value. The total load on the ith element can be written in the form

$$\eta_i = f + \sum_j V_{ij} \frac{1 + \sigma_j}{2}, \tag{1}$$

where $f = F/N$ is the direct load due to the external load and V_{ij} represents the load transferred from the jth element (in case it is broken). The breaking of the ith element with threshold h_i is determined according to $\sigma_i E_i > 0$ with the local field $E_i(\boldsymbol{\sigma}) \equiv (\eta_i - h_i)(1 - \bar{\sigma})/2$. This gives the stationary state at which the system eventually arrives.

For a more realistic description of the time evolution, we also take into consideration the uncertainty (noise) present in a real situation, which may arise from imperfections, random variations and other environmental influences. We thus consider the conditional probability that the ith element breaks at time $t + \delta t$, given that it is intact at time t

$$p(\sigma_i = +1, t + \delta t \mid \sigma_i = -1, t; \boldsymbol{\sigma}', t - t_d) = \frac{\delta t}{2t_r}[1 + \tanh \beta E_i'], \tag{2}$$

where $\boldsymbol{\sigma}' \equiv (\sigma_1', \sigma_2', \ldots, \sigma_N')$ represents the configuration of the system at time $t - t_d$ and $E_i' \equiv E_i(\boldsymbol{\sigma}')$ is the local field at time $t - t_d$. Note the two time scales t_d and t_r here: t_d denotes the time delay during which the load is redistributed among elements while the refractory period t_r sets the relaxation time (or lifetime). The 'temperature' $T \equiv \beta^{-1}$ measures the width of the threshold region of the elements or the noise level: in the noiseless limit ($T = 0$)

the factor $(1 + \tanh \beta E_i')/2$ in equation (2) reduces to the step function $\theta(E_i')$, yielding the stationary-state condition given above. We also assign the non-zero conditional probability of the ith element being repaired (healed) given that it is broken at time t:[5]

$$p(\sigma_i = -1, t + \delta t | \sigma_i = +1, t; \boldsymbol{\sigma}', t - t_d) = \frac{\delta t}{t_0}, \tag{3}$$

where t_0 is the time necessary for repairing. Equations (2) and (3) can be combined to give a general expression for the conditional probability $p(\sigma_i', t + \delta t | \sigma_i, t; \boldsymbol{\sigma}', t - t_d)$, which, in the limit $\delta t \to 0$, can be expressed in terms of the transition rate:

$$p(-\sigma_i, t + \delta t \mid \sigma_i, t; \boldsymbol{\sigma}', t - t_d) = w_i(\sigma_i; \boldsymbol{\sigma}', t - t_d)\delta t. \tag{4}$$

The transition rate is given by

$$w_i(\sigma_i; \boldsymbol{\sigma}', t - t_d) = \frac{1}{2t_r}\left[\left(a + \frac{1}{2}\right) + \left(a - \frac{1}{2}\right)\sigma_i + \frac{1 - \sigma_i}{2}\tanh \beta E_i'\right], \tag{5}$$

where the healing parameter $a \equiv t_r/t_0$ measures the repairing probability during the relaxation time. Here we point out that t_d, t_r, t_0 and accordingly a may be complicated functions of system properties like the average fraction of intact elements and others, which may be incorporated into the model. In this work we restrict ourselves to the simplest case of these parameters being fixed.

The behavior of the system is then governed by the master equation, which describes the evolution of the joint probability $P(\boldsymbol{\sigma}, t; \boldsymbol{\sigma}', t - t_d)$ that the system is in state $\boldsymbol{\sigma}'$ at time $t - t_d$ and in state $\boldsymbol{\sigma}$ at time t. In consequence equations describing the time evolution of relevant physical quantities, with the average taken over $P(\boldsymbol{\sigma}, t; \boldsymbol{\sigma}', t - 1)$, in general assume the form of differential-difference equations due to the delay in the load redistribution. For example, one may find the equation of motion for the average fraction of intact elements, $\bar{x} \equiv (2N)^{-1}\sum_k (1 - \langle\sigma_k\rangle) \equiv (2N)^{-1}\sum_k \sum_{\boldsymbol{\sigma},\boldsymbol{\sigma}'} P(\boldsymbol{\sigma}, t; \boldsymbol{\sigma}', t - 1)(1 - \sigma_k)$, which, in the case of global load sharing (GLS), leads to the self-consistency equation for the stationary solution [8, 12].

On the other hand, LLS, which is expected to generate nontrivial spatial correlations interrelated with temporal ones, does not grant analytical results. We thus resort to MC simulations, making use of equations (2) and (3). To this end, we place $N \equiv L^2$ elements at sites of a square lattice of linear size L under periodic boundary conditions. The algorithm to simulate the load transfer is as follows: (i) initially, all elements are intact, represented by $\sigma_i = -1$, and subject to equal load $f = F/L^2$. (ii) At each time step, the state of every element gets updated according to the probability given by equation (2) or (3), depending on its present state. The order of update is determined at random. (iii) When an element becomes broken ($\sigma_i = +1$), its load is transferred into the nearest and next nearest neighbors, i.e., elements on the 3×3 square centered at the broken element. Each intact neighbor receives an equal amount of the excess load. If there is no intact element on the first (3×3) square, the load is transferred to the intact elements on the second (5×5) square, and so on. If there is no intact element up to the tenth square of linear size 21, the load is shared by all intact elements in the system, each getting an equal amount. It is obvious that this is just one of the many possible ways to realize load sharing; we have considered several other realizations of local load sharing, to find that the behavior of the system does not change qualitatively. (iv) A healed (repaired) element gets its load from nearby intact elements in a similar manner. Namely, each intact neighbor chosen gives an equal amount of load to the repaired element, in such a way that the load on it is equal to the average load of the chosen elements before the

[5] Note that in the sandpile model healing is provided by external driving (input), which maintains criticality.

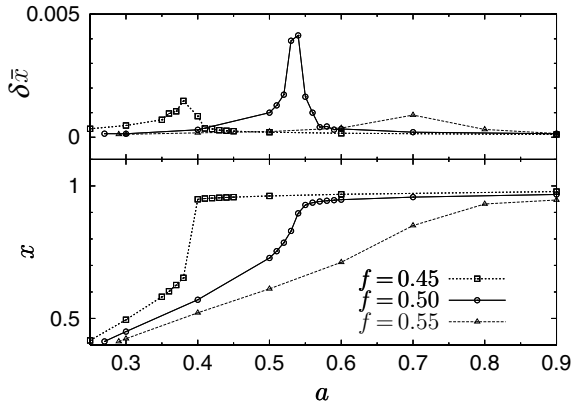

Figure 1. Average fraction $\bar{x}$ of intact elements (lower box) and its fluctuations $\delta\bar{x}$ (upper box) versus healing parameter a in the stationary state of a system with LLS, for several values of f at $T = 0.2$. Symbols represent data points obtained from MC simulations whereas lines are merely guides to the eye. Errors are smaller than the symbol sizes.

load transfer. (v) Measuring the average fraction $\bar{x}$ of intact elements completes the time step, comprising one MC sweep. (vi) At each time step, the number of newly broken elements is also counted, from which the breakage rate R_d is computed.

The threshold $\{h_i\}$ is assumed to follow a Gaussian distribution with mean $\bar{h}$ and standard deviation σ. Specifically, we set $\tau \equiv t_r/t_d = 5$, $\bar{h} = 1$ and $\sigma = 0.2$, and use the time step $\Delta t = 0.5$ in a system of size $L = 512$. These parameter values have been varied, only to give no qualitative difference. Most results of MC simulations presented in this work represent average values over 30 initial configurations.

Plotted in figure 1 are the average fraction $\bar{x}$ of intact elements (lower box) and its fluctuations $\delta\bar{x}$ estimated by standard deviations (upper box) versus the healing parameter a for several values of load f at the noise level $T = 0.2$. For small values of the load, e.g., $f = 0.45$ in figure 1, one observes an apparently discontinuous transition at $a \approx 0.4$; this is to be contrasted with the case of larger values of f, where $\bar{x}$ changes continuously with a. These behaviors are qualitatively the same as those of the system with GLS, where an analytical approach reveals a bistable region in some range of a, characterized by two stable solutions of $\bar{x}$ and an unstable one together with the associated hysteresis [13]. It is thus presumed that for small f in figure 1 there also exists a bistable region, where the fraction $\bar{x}$ jumps from one stable state to the other as the healing parameter a is varied. As f is increased, the bistable region shrinks and beyond the 'critical' load f_c, there exists only one state and $\bar{x}$ changes continuously with a. Note that for f below f_c fluctuations grow in the region of the discontinuous transition, becoming stronger than those for other values of f (compare data for $f = 0.45$ with those for $f = 0.5$ or 0.55 at $a \lesssim 0.4$) although data points shown for the latter cases are limited; nevertheless, they appear weaker than the fluctuations in the critical region of the system under $f = 0.5$.

Here spatial correlations may give rise to a power-law distribution, e.g., in the cluster sizes; such power-law distributions have also been reported in related models [14]. We therefore measure the size s of each cluster of broken elements in MC simulations and count the number n of clusters of size s. By a cluster, we mean a group of elements that are connected as neighbors in the same (broken) state. Figure 2 shows the obtained cluster size distribution at stationarity for several values of f and a (a) outside and (b) near the critical region. Power-law distributions

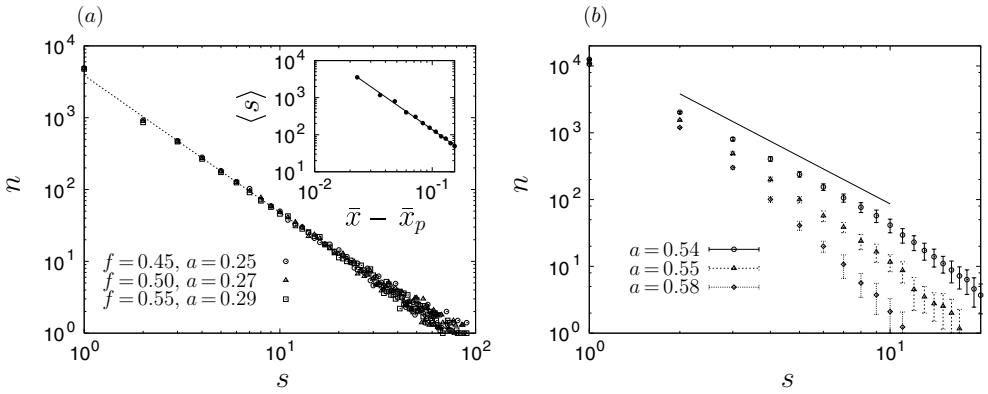

Figure 2. Cluster size distribution, i.e., number n of clusters of broken elements versus cluster size s in the stationary state of the system for (a) $(f, a) = (0.45, 0.25)$, $(0.50, 0.27)$ and $(0.55, 0.29)$; (b) $f = 0.5$ and $a = 0.54, 0.55$ and 0.58. While all data in (a) collapse into a single line of the slope $\alpha = 1.9$, obtained from the linear regression, in (b) only the data near the critical region $(a \approx 0.54)$ exhibit power-law behavior with $\alpha = 2.4$, represented by the line. The inset in (a) manifests the power-law behavior of the average cluster size $\langle s \rangle$ versus the deviation $\bar{x} - \bar{x}_p$ from the percolative critical fraction $\bar{x}_p = 0.415$ with the slope $\gamma = 2.2$.

of cluster sizes are observed: the number n of clusters of size s satisfies $n(s) \propto s^{-\alpha}$. In (a), data for all three different sets of (f, a) collapse into a single line, disclosing power-law behavior with the exponent $\alpha = 1.9(1)$. We have also examined the size distribution for other values of (f, a), to observe that the behavior apparently depends on the average fraction $\bar{x}$. Indeed the three sets of (f, a) in figure 2(a) all correspond to $\bar{x} = 0.415 \pm 0.005$, which, together with the exponent $\alpha \approx 2$, indicates the presence of percolation-type criticality at $\bar{x}_p = 0.415$. In addition, within error bars the exponent $\gamma = 2.2(2)$ in the average cluster size $\langle s \rangle \equiv \sum s^2 n(s) \big/ \sum s n(s) \propto |\bar{x} - \bar{x}_p|^{-\gamma}$ is also consistent with $\gamma = 43/18$ in the site percolation (see the inset). It is thus believed that the system under weak healing belongs to the percolation universality class. The difference from the value $1 - p_c = 0.407$ with the threshold probability $p_c = 0.593$ in the site percolation reflects correlations between sites present in our system. On the other hand, figure 2(b) shows that data near the critical region display power-law behavior with the exponent $\alpha = 2.4(1)$, up to the cutoff due to finite-size effects. This rather large exponent results from other mechanism than percolation and may be attributed to SOC-type criticality, since the local rule of LLS sustains the balance between breakage and healing in that region.

As for the time evolution, while the average fraction $\bar{x}$ in general decreases from unity and reaches the stationary state, the breakage rate R_d apparently exhibits complex behavior in the stationary state, which may be conveniently characterized by its power spectrum. When healing is weak, the overall power spectrum remains white although a region of power-law behavior develops at intermediate frequencies (unless $a = 0$). In contrast, the power-law behavior of the form $P(\omega) \propto \omega^{-\phi}$ is most prominent near the critical region of the discontinuous transition where healing is stronger, as displayed in figure 3 for $f = 0.50$. It is observed that the exponent ϕ reduces as a is increased beyond the critical value $a_c \approx 0.54$, where fluctuations are strongest (see figure 1). The large value of ϕ at a_c presumably results from the increase of the number of available states in the (f, a) parameter space. The system may then move around among many states via 'hopping' with the assistance of noise and induce collective breakage of many elements, which in turn causes the low-frequency components

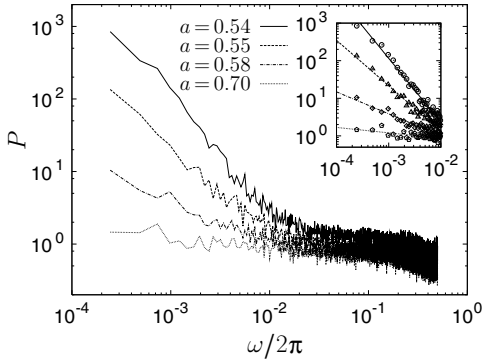

Figure 3. Power spectrum $P(\omega)$ of the breakage rate $R_d(t)$ in the stationary state of the same system as in figure 1 for $f = 0.5$. The exponent ϕ is given by 1.7, 1.2, 0.59 and 0.14 for $a = 0.54, 0.55, 0.58$ and 0.70, respectively (see the inset).

of the power spectrum to increase. The power-law behavior does not disappear completely as the load gets somewhat smaller ($f = 0.45$) or larger ($f = 0.55$) than the critical load (not shown), reminiscent of SOC-type criticality without fine tuning. The scale invariance in the power spectrum may be enhanced by the power law in the cluster size distribution of broken elements: since the breakage of a larger cluster is an event of lower frequency than that of a small cluster, the presence of many larger clusters should increase the power spectrum at smaller frequencies. Recall that healing is not weak in those regions where the power spectrum displays distinct power-law behavior; this reflects that an adequate amount of input is required to maintain SOC. This contrasts with the usual case of a phase transition where power-law behavior appears only at the transition point. On the other hand, the exponent varies with a and reaches a peak in the critical region ($a \approx a_c$) where strong fluctuations are present, indicating that the discontinuous transition comes into play. It is thus concluded that the criticality in temporal correlations arises from the interplay of the discontinuous transition and SOC, involved in spatial correlations.

Acknowledgments

This work was supported by the BK21 Program, MOST/KOSEF through NCRC for Systems Bio-dynamics (MYC), and 2006 Research Fund of University of Ulsan (BGY).

References

[1] Gutenberg B and Richter C F 1954 *Seismicity of the Earth and Associated Phenomenon* (Princeton, NJ: Princeton University Press)
[2] Raup D M 1986 *Science* **231** 1528
Raup D M and Boyajian G E 1988 *Paleobiology* **14** 109
Adami C 1995 *Phys. Lett.* A **203** 29
Vandewalle N and Ausloos M 1995 *Europhys. Lett.* **32** 613
Fernandez J, Plastino A and Diambra L 1995 *Phys. Rev.* E **52** 5700
[3] Albert R and Barabasi A-L 2002 *Rev. Mod. Phys.* **74** 47
[4] Glodberger A L *et al* 1999 *Nature* **399** 461
Scheinkman J A and Woodford M 1994 *Am. Econ. Rev.* **84** 417
[5] Bak P, Tang C and Wiesenfeld K 1987 *Phys. Rev. Lett.* **59** 381
Bak P, Tang C and Wiesenfeld K 1988 *Phys. Rev.* A **38** 364

[6] Bak P and Tang C 1989 *J. Geophys. Res.* **94** 15635
Drossel B and Schwabl F 1992 *Phys. Rev. Lett.* **69** 1629
Bak P and Sneppen K 1993 *Phys. Rev. Lett.* **71** 4083
Ito K 1995 *Phys. Rev.* E **52** 3232
See also Choi M Y, Kim B J, Yoon B-G and Park H 2005 *Europhys. Lett.* **69** 503
[7] Zapperi S, Ray P, Stanley H E and Vespignani A 1997 *Phys. Rev. Lett.* **78** 1408
[8] Choi J, Choi M Y and Yoon B-G 2005 *Europhys. Lett.* **71** 501
[9] See, e.g., da Silveira R 1999 *Am. J. Phys.* **67** 1177
[10] Andersen J V, Sornette D and Leung K-T 1997 *Phys. Rev. Lett.* **78** 2140
Zhang S D 1999 *Phys. Rev.* E **59** 1589
Newman W I and Phoenix S L 2001 *Phys. Rev.* E **63** 021507
[11] Scorretti R, Ciliberto S and Guarino A 2001 *Europhys. Lett.* **55** 626
Moral L, Moreno Y, Gomez J B and Pacheco A F 2001 *Phys. Rev.* E **63** 066106
Pradhan S, Bhattacharyya P and Chakrabarti B K 2002 *Phys. Rev.* E **66** 016116
Choi M Y, Choi J and Yoon B-G 2004 *Europhys. Lett.* **66** 62
Kim B J 2004 *Europhys. Lett.* **66** 819
[12] Yoon B-G, Choi J and Choi M Y 2005 *J. Korean Phys. Soc.* **47** 1053
Yoon B-G, Choi J, Choi M Y and Fortin J-Y 2006 *Phys. Rev.* E **73** 031905
[13] Kang H, Jo J, Choi M Y, Choi J and Yoon B-G 2007 *J. Phys. A: Math. Theor.* **40** 3319
[14] Pradhan S and Chakrabarti B K 2001 *Phys. Rev.* E **65** 016113
Hidalgo R C, Moreno Y, Kun F and Herrmann H J 2002 *Phys. Rev.* E **65** 046148